

# Fate of Rising CO<sub>2</sub> Droplets in Seawater

YOUXUE ZHANG<sup>\*,†,‡</sup>

Department of Geological Sciences, The University of Michigan, Ann Arbor, Michigan 48109-1005, USA; and Key Laboratory of Orogenic Belts and Crustal Evolution, MOE, School of Earth and Space sciences, Peking University, Beijing, 100871, China

The sequestration of fossil fuel CO<sub>2</sub> in the deep ocean has been discussed by a number of workers, and direct ocean experiments have been carried out to investigate the fate of rising CO<sub>2</sub> droplets in seawater. However, no applicable theoretical models have been developed to calculate the dissolution rate of rising CO<sub>2</sub> droplets with or without hydrate shells. Such models are important for the evaluation of the fate of CO<sub>2</sub> injected into oceans. Here, I adapt a convective dissolution model to investigate the dynamics and kinetics of a single rising CO<sub>2</sub> droplet (or noninteracting CO<sub>2</sub> droplets) in seawater. The model has no free parameters; all of the required parameters are independently available from literature. The input parameters include: the initial depth, the initial size of the droplet, the temperature as a function of depth, density of CO<sub>2</sub> liquid, the solubility of CO<sub>2</sub> liquid or hydrate, the diffusivity of CO<sub>2</sub>, and viscosity of seawater. The effect of convection in enhancing mass transfer is treated using relations among dimensionless numbers. The calculated dissolution rate for CO<sub>2</sub> droplets with a hydrate shell agrees with data in the literature. The theory can be used to explore the fate of CO<sub>2</sub> injected into oceans under various temperature and pressure conditions.

## Introduction

The disposal of fossil fuel CO<sub>2</sub> in the deep ocean has been considered as a possible means to mitigate the growth of greenhouse gas in the atmosphere (1–5). Much work has been carried out on injection schemes (2–5). To evaluate the consequences (including safety and environmental effects, e.g., ref 6) of CO<sub>2</sub> injection, it is critical to understand the fate of injected CO<sub>2</sub> at different levels of ocean water. Recently, Brewer et al. (7, 8) carried out particularly useful direct experiments on the ocean disposal of fossil CO<sub>2</sub>. They monitored the dissolution of two rising CO<sub>2</sub> droplets (both having an initial radius of 4.55 mm) with hydrate shells by in situ ocean experiments. However, a theoretical understanding of the dissolution data is still lacking. Such an understanding is important to evaluate the dissolution rate and fate of rising or falling CO<sub>2</sub> droplets in seawater under various temperature (*T*) and pressure (*P*) conditions.

Models on crystal or bubble dissolution (9–11) cited by Brewer et al. (8) either are for dissolution under different hydrodynamic conditions or are empirical with a free fitting

parameter. The dissolution model of Broecker and Peng (9) and the hydrodynamic model of Opdyke et al. (12) with confirmation by direct measurement of alabaster dissolution by Santschi et al. (10) are for dissolution of minerals on the seafloor in the presence of a current and do not apply to the hydrodynamics of dissolution of rising CO<sub>2</sub> droplets in water. The bubble dissolution model of Leifer et al. (11) has an empirical parameter. Because of difficulties in calculating the dissolution rate of droplets from first principles, workers modeled experimental data on the rising velocity (8, 13), but did not model dissolution rates. One apparent exception was the work of Brewer et al. (8). In their work, after presenting experimental data on the rising velocity and dissolution rate of rising liquid CO<sub>2</sub> droplets with a thin hydrate shell, they mentioned the standard model for dissolution rates in the oceans (9, 10). They estimated the boundary layer thickness next to a rising droplet at 0.12 m/s to be 300 μm, based on a reported boundary layer thickness of 500 μm over a horizontal bed for a velocity of 0.08 m/s (10). The method of estimation is incorrect because the hydrodynamic condition for a rising droplet differs from that for a horizontal bed with overlying flow. It will be shown later that the value of boundary layer thickness is also incorrect. Brewer et al. (8) nonetheless did not use the estimated boundary layer thickness to model the dissolution rate of the rising CO<sub>2</sub> liquid droplets. Instead, they first fit the data of droplet diameter versus time to obtain the dissolution rate (their Figure 5), and then calculated the droplet size decrease “based upon the measured dissolution rate” (their Figure 6). That is, their modeling of droplet size versus time is circular and does not constitute a model for dissolution rate of liquid CO<sub>2</sub> droplets.

In a series of developments (14–17) mostly by the high-temperature geochemical community, a convective dissolution model has been developed (17) to calculate the dissolution rate of a freely rising or falling crystal in magma or water without any free parameters. The model was confirmed by experimental data (17). Herzog et al. (2) also developed a convective dissolution model for liquid droplets of CO<sub>2</sub>. Although the model of Herzog et al. (2) and that of Zhang and Xu (17) are similar in terms of general approaches, Herzog et al. employed four sets of velocity/mass transfer relations to produce four sets of results, none of which is confirmed experimentally.

In this contribution, the model of ref 17 is adapted to investigate the fate of rising CO<sub>2</sub> droplets in seawater, to explore the behavior of CO<sub>2</sub> droplets under various temperature and pressure conditions in oceans, and to evaluate the safety of CO<sub>2</sub> injections into oceans. In the stability field of CO<sub>2</sub> hydrate, a hydrate shell forms on CO<sub>2</sub> droplet due to reaction of liquid CO<sub>2</sub> with seawater at the interface. This hydrate shell is expected to be very thin because it dissolves in seawater as it grows in a delicate steady state. With a thin hydrate shell, the dissolution rate during the rise or fall of a CO<sub>2</sub> droplet can be modeled in a fashion similar to the dissolution rate of a falling or rising crystal. The density of the droplet is still the liquid density because the hydrate shell is thin, but the CO<sub>2</sub> solubility is that of CO<sub>2</sub> hydrate, which is lower than that of CO<sub>2</sub> liquid (otherwise hydrate would not form). Hence, the formation of the hydrate shell reduces the dissolution rate. The convective dissolution model calculates both the ascent velocity and the dissolution rate without any empirical fitting parameters. The input parameters include: the initial conditions (such as the initial depth and the initial size of the droplet), and the surrounding conditions (such as the temperature and seawater density), as well as other parameters that are independently measured

\* Corresponding author phone: (734)763-0947; fax: (734)763-4690; e-mail: youxue@umich.edu.

† The University of Michigan.

‡ Peking University.

or obtainable, such as the density of the CO<sub>2</sub> droplet, the solubility of CO<sub>2</sub> in water (depending on whether there is a hydrate shell), and CO<sub>2</sub> diffusivity in and viscosity of water (both depending on temperature). The effect of convection in enhancing mass transfer is considered rigorously using relations among dimensionless numbers. The input parameters must be gathered from literature and interpolated or extrapolated to the necessary conditions in oceans based on known principles. With these parameters and conditions, the dissolution rate for a rising or sinking CO<sub>2</sub> droplet can be calculated. The theory is applicable to a single droplet rising or falling in an infinite fluid medium and to noninteracting droplets (i.e., the diffusion profile next to one droplet does not overlap with that next to any neighboring droplet).

Below, the previous model is extended as necessary for the specific case of dissolution of CO<sub>2</sub> droplets with or without a hydrate shell. The theory is then applied to calculate and compare with dissolution rates in the direct ocean experiments of Brewer et al. (8). Fate of rising or sinking CO<sub>2</sub> droplets in the context of CO<sub>2</sub> sequestration in oceans is then discussed.

### Theory for Convective Dissolution of a Rising Liquid CO<sub>2</sub> Droplet With or Without a Thin Hydrate Shell

The following development follows that of ref 17. Below, the subscript “w” means either pure water or seawater. The subscript “liq” means CO<sub>2</sub> liquid. For convective dissolution of a liquid CO<sub>2</sub> droplet as it buoyantly rises or falls through seawater, mass transfer is enhanced and typically dominated by forced convection due to buoyant descent or ascent of the droplet. The motion of the droplet induces a flow field, and the flow removes water next to the droplet, resulting in a thin compositional boundary layer next to the dissolving droplet. The boundary layer thickness is thinner on the leading side of the droplet and thicker on the trailing side. Although the thickness of the boundary layer is variable on different sides of the moving droplet, an effective boundary layer thickness ( $\delta_c$ , where the subscript “c” means compositional) is defined, and the convective dissolution rate may be modeled as:

$$-da/dt = \beta_c D / \delta_c \quad (1)$$

where  $a$  is the radius of the droplet,  $-da/dt$  is the dissolution rate (note that  $da/dt$  is negative as  $a$  decreases with time),  $D$  is the diffusivity of dissolved CO<sub>2</sub> in water, and  $\beta_c$  is a dimensionless parameter defined as

$$\beta_c = (C_{\text{sat}} - C_{\infty}) / (C_{\text{CO}_2(\text{liq})} - C_{\text{sat}}) \quad (2)$$

where  $C_{\text{sat}}$  is the concentration (solubility) of CO<sub>2</sub> at the interface water at saturation,  $C_{\infty}$  is the CO<sub>2</sub> concentration in ambient water (usually zero), and  $C_{\text{CO}_2(\text{liq})}$  is the CO<sub>2</sub> concentration in the liquid droplet to be dissolved (that is, density of CO<sub>2</sub> in the whole droplet); all concentrations are in mol/L, and  $\beta_c$  is dimensionless. Note that  $C_{\text{sat}}$  in the above equation depends on whether a thin hydrate shell forms on the CO<sub>2</sub> droplet. Without a hydrate shell,  $C_{\text{sat}}$  is the saturation CO<sub>2</sub> concentration in seawater in equilibrium with liquid CO<sub>2</sub>. If a shell forms,  $C_{\text{sat}}$  is the saturation CO<sub>2</sub> concentration corresponding to hydrate solubility. However,  $C_{\text{CO}_2(\text{liq})}$  is not affected by the formation of a thin hydrate shell because the bulk of the droplet is still liquid and the density of the droplet is hence unaffected. Equation 1 applies to both diffusive and convective dissolution (14).

$D$  is available from literature, and  $\beta_c$  can be estimated from solubility and CO<sub>2</sub> liquid density (Appendix). Hence, the problem of calculating the dissolution rate according to eq 1 becomes the problem of obtaining the average boundary layer thickness  $\delta_c$ . For forced convection due to free buoyant

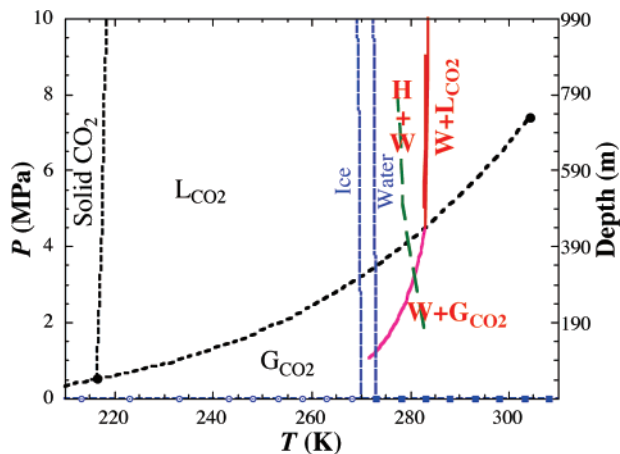


**FIGURE 1.** Phase diagram of the CO<sub>2</sub> system and the CO<sub>2</sub>-H<sub>2</sub>O system. The dashed black curves mark phase boundaries for pure CO<sub>2</sub>. The phases in the pure CO<sub>2</sub> system are marked in black. The dashed blue curves (and blue squares and dotted circles almost overlapping the horizontal axis) show phase boundaries of CO<sub>2</sub>-free “pure” seawater system. The phases in “pure” seawater system are marked in blue. The double blue lines are due to the variability of melting point from pure water to seawater. The solid red-purple curves mark phase boundaries in the CO<sub>2</sub>-H<sub>2</sub>O system. The phases in the CO<sub>2</sub>-H<sub>2</sub>O system are marked in red. Between the double blue lines and the solid red-purple curve, there are two phases: hydrate and liquid water (H+W). Between the red solid curve and the dashed black curve, there are two phases, liquid water and liquid CO<sub>2</sub> (W+L<sub>CO2</sub>). On the right-hand side of the purple curve, the two phases are liquid water and gas CO<sub>2</sub> (W+G<sub>CO2</sub>). The green curve shows a measured temperature-depth profile in the ocean (8).

rise or fall of a droplet,  $\delta_c$  can be estimated from the Sherwood number ( $Sh$ ), which in turn can be estimated from the compositional Peclet number  $Pe_c$  and the Reynold number  $Re$ . The dimensionless numbers are defined as:

$$Re = \frac{(2a)u\rho_w}{\mu_w} \quad (3)$$

$$Pe_c = 2au/D \quad (4)$$

$$Sh = 2a/\delta_c \quad (5)$$

where  $\rho_w$  and  $\mu_w$  are the density and viscosity of seawater, and  $u$  is the ascent or descent velocity of the droplet. For  $Re \leq 10^5$ , the three dimensionless parameters are related as follows for a rising or falling sphere (17):

$$Sh = 1 + (1 + Pe_c)^{1/3} \left( 1 + \frac{0.096 Re^{1/3}}{1 + 7 Re^{-2}} \right) \quad (6)$$

With the above theoretical development, the procedure for calculating the rising velocity and dissolution rate of a CO<sub>2</sub> droplet is as follows:

(i) Collect all necessary data as a function of  $T$  and  $P$ , including  $\mu_w$ ,  $\rho_w$ ,  $C_{\text{CO}_2(\text{liq})}$ , and  $\rho_{\text{CO}_2(\text{liq})}$  (both are density of CO<sub>2</sub> liquid but expressed in different units,  $C$  in mol/L and  $\rho$  in kg/m<sup>3</sup>),  $C_{\text{sat}}$  (solubility of CO<sub>2</sub> liquid in seawater, or solubility of CO<sub>2</sub> hydrate in seawater for shelled droplets), and  $D$  (diffusivity of dissolved CO<sub>2</sub> in seawater). The Appendix summarizes the various data.

(ii) Specify the initial depth and the variation of density and  $T$  with depth. Estimate  $P$ . Determine the stable phase of CO<sub>2</sub> under the given  $T$ - $P$  condition using the phase diagram of CO<sub>2</sub>-H<sub>2</sub>O (Figure 1). If CO<sub>2</sub> gas is stable, then the problem is bubble dissolution, which will be discussed in a

future contribution. If CO<sub>2</sub> liquid is stable, then the problem is droplet dissolution, which is addressed in this work, but the effect of wobbling and breakup is ignored. If CO<sub>2</sub> hydrate is stable, then a hydrate shell will form on a released CO<sub>2</sub> liquid droplet, which is also considered in this work. If CO<sub>2</sub> hydrate is released into seawater where CO<sub>2</sub> hydrate is stable, then the problem is crystal dissolution, which has been treated by Zhang and Xu (17) and can be treated using the procedures summarized here. The dissolution parameter  $\beta_c$  is calculated from the appropriate density ( $C_{CO_2(liq)}$ ) and solubility ( $C_{sa}$ ). The Appendix summarizes the calculation of  $\beta_c$ .

(iii) Given the density and radius of the droplet, calculate the ascent or descent velocity  $u$ . For  $Re < 1$ , use Stokes' law:  $u = 2ga^2\Delta\rho/(9\mu_w)$ , where  $g$  is acceleration due to Earth's gravity, and  $\Delta\rho$  is the density difference between seawater and liquid CO<sub>2</sub>. If  $Re > 1$ , Stokes' law is not applicable. For  $Re \leq 3 \times 10^5$ , three unknowns ( $u$ ,  $Re$ , and  $C_D$ ) may be solved iteratively from the following three equations:

$$Re = \frac{(2a)u\rho_w}{\mu_w} \quad (3)$$

$$C_D = \frac{24}{Re}(1 + 0.15Re^{0.687}) + \frac{0.42}{1 + 42500Re^{-1.16}} \quad (7)$$

$$u = \sqrt{\frac{8ga\Delta\rho}{3\rho_w C_D}} \quad (8)$$

Equation 7 is from ref 18, and the relative error is +6% to -4% for  $Re \leq 3 \times 10^5$ . Strictly speaking, eq 7 is applicable only to rigid spheres and hence is applicable to a liquid CO<sub>2</sub> droplet with a hydrate shell. Experience shows that it is also applicable to small drops and bubbles (13, 19), which is typically attributed to surfactants at the interfaces. Two notes are in order: (a) If  $Re$  is between  $1 \times 10^5$  and  $3 \times 10^5$ ,  $u$  may be calculated from the above procedure, but the dissolution rate cannot be calculated because eq 6 is derived using data for  $Re \leq 10^5$ , and its application to  $Re > 10^5$  is not guaranteed. (b) Brewer et al. (8) substituted  $\rho_{CO_2(liq)}$  for  $\rho_w C_D$  in eq 8 to calculate the rising velocity, which does not require iteration. It turns out that fortuitously  $\rho_{CO_2(liq)}$  and  $\rho_w C_D$  are similar under the conditions of investigation by ref 8, leading to their correct prediction of the rising velocity. However, their equation is inaccurate and should not be generally applied.

(iv) With the above results,  $Pe_c$  can be calculated from eq 4, and  $Sh$  can then be calculated from eq 6. The value of  $\delta_c$  is calculated from  $\delta_c = (2a)/Sh$  (eq 5). The dissolution rate is calculated from eq 1.

(v) The radius  $a$  of the droplet (with or without shell) is solved by integrating  $da/dt$ , that is,  $a = a_0 - \int(\beta_c D/\delta_c) dt$ . Depth is solved by integrating  $u$  with respect to  $t$ , that is,  $h = h_0 - \int u dt$ .

Because of the interdependence of  $a$ ,  $u$ ,  $Re$ ,  $Pe_c$ ,  $Sh$ , and  $\delta_c$ , the integrations can only be carried out numerically. In this work, the integration is carried out using a spreadsheet program. Estimated relative uncertainty of the calculation is up to 10% due to (a) uncertainties associated with the imperfect expressions for  $C_D$  and  $Sh$ , and (b) uncertainties in the input parameters, especially in the calculated CO<sub>2</sub> solubility of hydrate (see Appendix).

### Comparison with Experimental Data

Although the above kinetic and dynamic model treats both the rising (or falling) velocity and the dissolution rate, the discussion below focuses on the dissolution rate because the rising velocity has been modeled before (8, 13). Brewer et al. (8) measured dissolution rate of freely rising CO<sub>2</sub> droplets

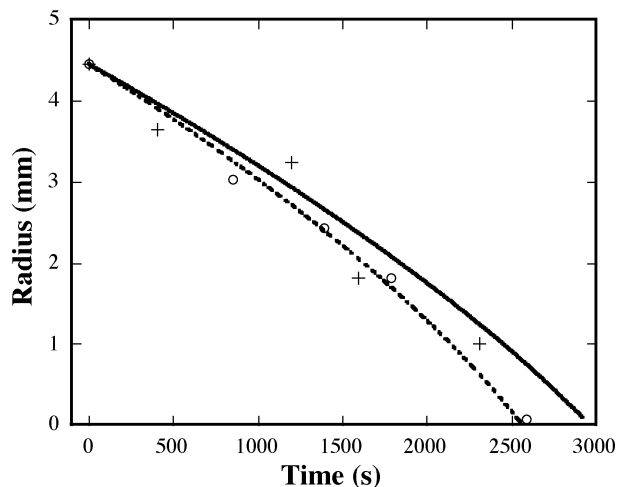


**FIGURE 2.** Comparison of experimental data of bubble radius versus time and calculations. Circles and pluses are experimental data from ref 8 using the same symbols they used, and the solid and dashed curves are the calculated bubble dissolution as a function of time for the two droplets. The two curves are slightly different due to the difference in initial depth and in temperature. The calculations are in good agreement with experimental data.

with a thin hydrate shell from about 800 m depth to about 400 m depth in the open ocean. At an average temperature of 278.35 K and 600 m (6.13 MPa), they determined a dissolution rate to be  $3.0 \mu\text{mol cm}^{-2} \text{s}^{-1}$ , which can be converted to a linear dissolution rate of  $1.44 \mu\text{m/s}$  ( $3.0 \times 10^{-6} \text{ mol cm}^{-2} \text{s}^{-1} \times 48 \text{ cm}^3/\text{mol} = 1.44 \times 10^{-4} \text{ cm/s} = 1.44 \mu\text{m/s}$ , where  $48 \text{ cm}^3/\text{mol}$  is the molar volume of liquid CO<sub>2</sub>). Using the convective dissolution theory, the linear dissolution rate can be calculated to be  $1.45 \mu\text{m/s}$  using  $\beta_c = 0.0504$  for a shelled CO<sub>2</sub> droplet (Appendix),  $D = 1160 \mu\text{m}^2/\text{s}$  at 278.35 K, and a boundary layer thickness  $\delta_c = 40.2 \mu\text{m}$  calculated from  $Re$ ,  $Pe_c$ , and  $Sh$  with an average radius of 3 mm. The calculated dissolution rate of  $1.45 \mu\text{m/s}$  is in excellent agreement with the experimental dissolution rate of  $1.44 \mu\text{m/s}$ . Again, it is emphasized that there is no fitting parameter in calculating the dissolution rate. The inferred boundary layer thickness surrounding the rising liquid CO<sub>2</sub> sphere is  $40 \mu\text{m}$ , much thinner than the incorrect estimate of  $300 \mu\text{m}$  by Brewer et al. (7), who applied hydrodynamics of an inappropriate regime. This shows that the correct hydrodynamic regime must be used to estimate the boundary layer thickness.

To further compare with the experimental data of Brewer et al. (8), droplet radius as a function of time and depth is calculated along the oceanic hydrotherm reported in Brewer et al. (8). Figure 2 compares calculated results along the oceanic hydrotherm with measured droplet size versus time data (8), and the agreement is very good. The two curves are slightly different because the initial depths and hence temperatures of the two droplets are slightly different (one droplet began its ascent from 804 m depth and 4.4 °C, and the other began its ascent from 649 m depth and 5.0 °C). The small difference between the theoretical calculation and experimental data can be attributed to uncertainties in the calculation and in the data.

The success of the above calculations shows that the kinetic/hydrodynamic model is accurate enough to have predictive power. It also shows that the solubility models of liquid CO<sub>2</sub> and CO<sub>2</sub> hydrate as a function of temperature and pressure as summarized in the Appendix are accurate enough to calculate the dissolution rate to an accuracy of about 10% relative.

## Dependence of Dissolution Rate on the Droplet Size, Temperature, and Pressure

With confirmation of the above theoretical model, the dissolution rate of CO<sub>2</sub> droplet in oceans at any depth and any temperature may be calculated. In addition to comparison with experimental data, theoretical calculations are carried out to examine the systematics of CO<sub>2</sub> droplet dissolution. The results show:

(1) The dissolution rate (or the boundary layer thickness) does not vary significantly with the radius of a CO<sub>2</sub> droplet. For example, for a given  $T$  and  $P$  (278 K and 670 m depth), when the radius of a CO<sub>2</sub> droplet varies by a factor of 10 from 5 to 0.5 mm, the boundary layer thickness decreases from 44.2 to 31.6  $\mu\text{m}$ , and the dissolution rate increases by only 40% from 1.26 to 1.77  $\mu\text{m/s}$ . Hence, if  $T$  and  $P$  were kept constant, the dissolution rate may be regarded as roughly constant and the radius of a droplet varies roughly linearly with time.

(2) The dissolution rate depends relatively strongly on temperature. For a droplet with a hydrate shell, increasing temperature increases the dissolution rate significantly because both  $D$  and  $\beta_c$  increase. The boundary layer thickness decreases slightly with increasing temperature because viscosity decreases. For a droplet without a hydrate shell, increasing temperature only increases the dissolution rate slightly because  $D$  increases but  $\beta_c$  decreases. For example, for a CO<sub>2</sub> droplet with a radius of 2 mm at a depth of 600 m, when the temperature varies from 274 to 280 K, the dissolution rate increases from 0.90 to 1.89  $\mu\text{m/s}$  (more than a factor of 2) if there is a hydrate shell, but from 2.05 to 2.52  $\mu\text{m/s}$  (23% increase) if there is no hydrate shell (i.e., if hydrate shell formation were impeded by kinetics).

(3) The dissolution rate depends weakly on pressure. At 20–30 MPa (depending on temperature), CO<sub>2</sub> liquid density is the same as that of seawater. Shallower than the depth (i.e., at  $P < 20$  MPa or depth  $< 2000$  m), as pressure (or depth) increases under constant temperature, the boundary layer thickness  $\delta_c$  increases slightly because the density difference between liquid CO<sub>2</sub> and seawater diminishes. If there is a hydrate shell,  $\beta_c$  decreases as pressure increases. If there is no hydrate shell,  $\beta_c$  changes very little as pressure increases. Combining the effect of pressure on the boundary layer thickness and on  $\beta_c$ , the dissolution rate decreases with increasing pressure. For a CO<sub>2</sub> droplet with a radius of 2 mm at 277 K, as the pressure increases from 5 to 15 MPa, the dissolution rate decreases from 1.36 to 0.95  $\mu\text{m/s}$  if there is a hydrate shell, and from 2.36 to 1.79  $\mu\text{m/s}$  if there is no hydrate shell.

(4) The effect of hydrate shell on protecting CO<sub>2</sub> droplets is significant, especially at lower temperatures (further away from the hydrate formation temperature). For example, at 273 K and 600 m depth for a radius of 2 mm, the dissolution rate without hydrate shell (1.98  $\mu\text{m/s}$ ) is 2.5 times the rate with hydrate shell (0.79  $\mu\text{m/s}$ ). Both the temperature and the hydrate effects can also be seen from experimental data (20).

If CO<sub>2</sub> droplets were injected deep enough so that they would sink, they also would undergo dissolution as they fall, and the rates can be calculated using the same equations except that the depth increases as the droplet falls freely and dissolves. Figure 3 shows the calculated fate of falling shelled CO<sub>2</sub> droplets. A droplet of 5 mm radius may survive a water column of more than 300 m, and that of radius 10 mm may survive a water column of 1600 m. On the seafloor, a CO<sub>2</sub> liquid or hydrate layer would dissolve gradually.

The dissolution rate of a seafloor CO<sub>2</sub> hydrate layer, or a layer of CO<sub>2</sub> liquid coated by a thin hydrate film, may be calculated using eq 10 in ref 17; the formulation in ref 10 is not used because it only applies to small length scales (such

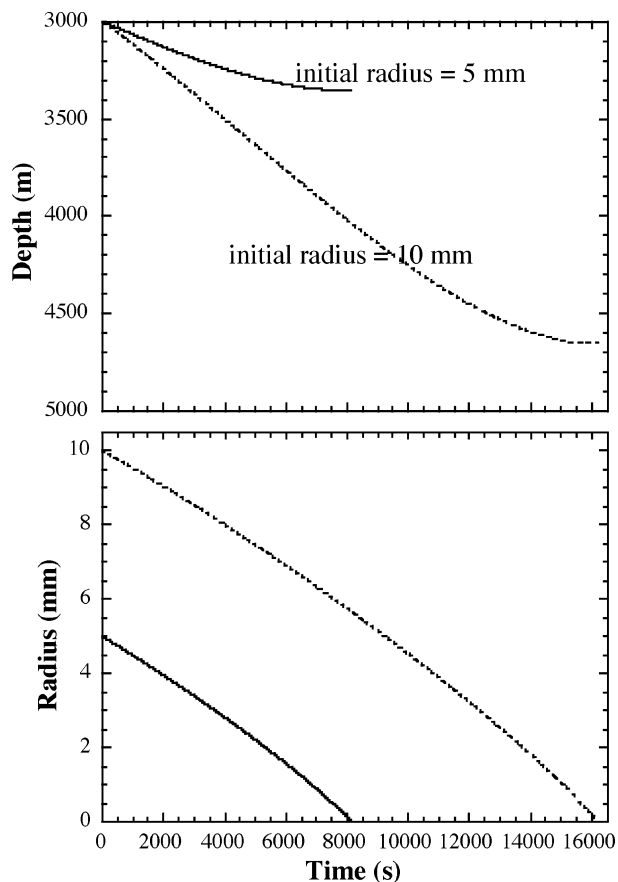


**FIGURE 3.** Calculated falling and dissolution history for two CO<sub>2</sub> droplets in seawater with a temperature of 275 K, density of 1026 kg/m<sup>3</sup>, and salinity of 35‰. Both started at a depth of 3000 m (hence they fall in seawater). The initial radius of one droplet is 5 mm, and that of the other is 10 mm.

as 1 m or less). For a depth of 3000 m and a temperature of 275 K,  $\beta_c$  for liquid CO<sub>2</sub> with hydrate shell is 0.0332,  $D = 1.05 \times 10^{-9} \text{ m}^2/\text{s}$ ,  $\mu = 0.00179 \text{ Pa s}$ . For  $\rho_w = 1026 \text{ kg/m}^3$ ,  $u = 0.05 \text{ m/s}$ , and a length scale of 1000 m, the dissolution rate is about 0.011  $\mu\text{m/s}$  (or 0.35 m/yr) using eq 10 of ref 17. A 100-m layer would dissolve in about 300 years. If the whole liquid CO<sub>2</sub> layer reacts to become a hydrate layer before dissolution, the layer thickness would increase, and  $\beta_c$  would increase roughly proportionally (Appendix). Hence, the same mass of CO<sub>2</sub> would take roughly the same time to dissolve.

## Discussion

Avoiding CO<sub>2</sub>-driven eruptions (21–23) from CO<sub>2</sub> injected in oceans is obviously a consideration in any schemes for CO<sub>2</sub> disposal in oceans because it would defeat the purpose of CO<sub>2</sub> sequestration and could be a hazard. Starting from a depth of 800 m and a temperature of 5 °C, model calculations show that a CO<sub>2</sub> droplet of 5.5 mm radius would be able to rise to 400 m depth. Starting from a depth of 600 m, a CO<sub>2</sub> droplet of 4 mm in radius would be able to reach 400 m depth. If CO<sub>2</sub> droplets rise to the depth for CO<sub>2</sub> liquid to gas transition (at about 400 m depth), and hydrate dissociation depth (350 m), then CO<sub>2</sub> bubbles would form. If furthermore the CO<sub>2</sub> quantity is very large and bubbles are highly concentrated, the resulting CO<sub>2</sub> bubble plume could erupt, with dynamics similar to that of lake eruptions (24) or the hypothesized, methane driven, ocean eruptions (25). Moreover, if a large amount of CO<sub>2</sub> liquid is injected into seawater, depending on the density difference between CO<sub>2</sub> liquid and seawater, the number density of droplets (number of droplets per unit volume of seawater), and the size of the

droplets, there would be a critical condition under which the system becomes unstable and the parcel of seawater containing numerous droplets may rise as a plume. This rapid rise into shallow seawater may lead to rapid CO<sub>2</sub> gas formation, which under the appropriate conditions may also lead to CO<sub>2</sub>-driven water eruptions.

To avoid the formation of rising CO<sub>2</sub> droplet plumes, and to avoid CO<sub>2</sub>-driven eruptions, injection of CO<sub>2</sub> liquid into the shallow oceans needs to be controlled, using low injection rates and dispersing CO<sub>2</sub> liquid to a large volume of seawater. Safer injection schemes (but not in terms of the acidity of the ocean) include: (i) injection of CO<sub>2</sub> liquid to great enough depths that liquid CO<sub>2</sub> density is greater than ambient seawater (e.g., at depth of >2000 m at 272 K and >3000 m at 281.8 K for seawater density of 1026 kg/m<sup>3</sup>) so that CO<sub>2</sub> liquid would sink and gradually dissolve in seawater, or (ii) dissolution of CO<sub>2</sub> gas in seawater to be brought down by thermohaline circulation (1).

### Acknowledgments

I acknowledge the US NSF and the donors of the American Chemical Society Petroleum Research Fund for partial support of this research. I thank Eric Essene and two anonymous reviewers for their insightful comments.

### Appendix: Values of Various Parameters for Liquid CO<sub>2</sub>

In this Appendix, estimations of various input parameters are summarized. The molecular mass of CO<sub>2</sub> is 0.04401 kg/mol. Angus et al. (25) summarized the properties of pure CO<sub>2</sub>. The density of liquid CO<sub>2</sub> depends on *T* and *P* and can be found in Angus et al. (25). At 800 m depth (*P* = 8.14 MPa) and 277.55 K, the density of liquid CO<sub>2</sub> is about 938 kg/m<sup>3</sup>, the molar volume of CO<sub>2</sub> is 0.0469 L/mol, and the concentration of CO<sub>2</sub> in liquid CO<sub>2</sub> is *C*<sub>CO<sub>2</sub></sub> = 21.32 mol/L. The CO<sub>2</sub> pressure for liquid CO<sub>2</sub> formation is based on data in Angus et al. (25) and is given as a function of temperature as follows:

$$\ln\left(\frac{P_{\text{sat}}}{P_c}\right) = a_0\left(1 - \frac{T}{T_c}\right)^{1.935} + a_1\left(\frac{T_c}{T} - 1\right) + a_2\left(\frac{T_c}{T} - 1\right)^2 + a_3\left(\frac{T_c}{T} - 1\right)^3 + a_4\left(\frac{T_c}{T} - 1\right)^4 \quad (\text{A1})$$

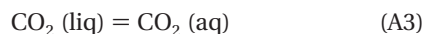
where *P*<sub>sat</sub> is the two-phase equilibrium pressure between liquid and gas CO<sub>2</sub>, *T* is temperature in K, *T*<sub>c</sub> and *P*<sub>c</sub> are the temperature and pressure at the critical point (*T*<sub>c</sub> = 304.21 K, *P*<sub>c</sub> = 7.3825 MPa), *a*<sub>0</sub> = 11.377371, *a*<sub>1</sub> = -6.8849249, *a*<sub>2</sub> = -9.5924263, *a*<sub>3</sub> = 13.679755, and *a*<sub>4</sub> = -8.6056439. The latent heat of liquid CO<sub>2</sub> vaporization is roughly 2560(*T*<sub>c</sub> - *T*)<sup>0.4</sup> J/mol (25). The heat capacity of liquid CO<sub>2</sub> at 280 K is taken to be 105 J/mol/K.

The diffusivity of CO<sub>2</sub> in seawater is assumed to be the same as that in pure water and is expressed as (26):

$$D_{\text{CO}_2} = \exp(-12.462 - (2258.5/T)) \quad (\text{A2})$$

where *D*<sub>CO<sub>2</sub></sub> is in m<sup>2</sup>/s. Seawater is assumed to have a salinity of 35‰ and a density of 1026 kg/m<sup>3</sup> unless otherwise specified.

The solubility of H<sub>2</sub>O in liquid CO<sub>2</sub> is vanishingly small (8) and ignored. The calculation of the solubility of CO<sub>2</sub> gas, liquid, and hydrate in seawater is the most complicated step in the dissolution model. The solubility of CO<sub>2</sub> gas in seawater (27, 28) is calculated from the model of ref 27. For solubility of CO<sub>2</sub> liquid in seawater, the following reaction is considered:



The equilibrium constant for the above reaction is *K* =

**TABLE 1. Estimation of β<sub>c</sub> for the Dissolution of CO<sub>2</sub> Droplets (No Shell) in Seawater**

temp (K)	depth (m)	density of CO <sub>2</sub> liquid (kg/m <sup>3</sup> )	solubility <i>C</i> <sub>sat</sub> (mol/L)	<i>C</i> <sub>liquid</sub> (mol/L)	β <sub>c</sub>
277.55	800	938	1.55	21.32	0.0782
278.35	600	916	1.51	20.82	0.0780
279.5	400	886	1.46	20.14	0.0780
277.55	3000	1041	1.75	23.65	0.0799
275	3000	1049	1.82	23.84	0.0826

*C*<sub>CO<sub>2</sub>(aq) sat</sub>, where *C*<sub>CO<sub>2</sub>(aq) sat</sub> is CO<sub>2</sub> solubility in seawater in equilibrium with liquid CO<sub>2</sub>. To estimate *K* at a given *T* and *P*, recall that the solubility of liquid CO<sub>2</sub> in seawater at *P*<sub>sat</sub> (vapor pressure of the liquid) for that *T* equals that of CO<sub>2</sub> gas in seawater at *T* and *P*<sub>sat</sub>. At the same *T* and higher *P* (in the CO<sub>2</sub> liquid field), ln *K* would then change with pressure as -∫Δ*V* d*P*/(*RT*), in which Δ*V* = *V*<sub>CO<sub>2</sub>(aq)</sub> - *V*<sub>CO<sub>2</sub>(liq)</sub>, where *V*<sub>CO<sub>2</sub>(aq)</sub> = 0.0323 L/mol (27), and *V*<sub>CO<sub>2</sub>(liq)</sub> is obtained from ref 25. At 800 m (8.145 MPa) and 277.55 K, Δ*V* ≈ -0.0146 L/mol, meaning that ln *K* would increase by 0.15 as *P* increases from 4 to 30 MPa (about 3000 m depth) at 277.55 K. That is, the effect of pressure on CO<sub>2</sub> liquid solubility is small, and hence the uncertainty in this calculation is assumed to be small. The solubility of CO<sub>2</sub> in seawater is smaller than that in pure water. For example, CO<sub>2</sub> solubility in seawater with a salinity of 35‰ is about 84% of that in pure water (27).

As an example, consider the solubility of CO<sub>2</sub> liquid in seawater at 4.4 °C and 800 m depth (*P* = 8.145 MPa) ignoring hydrate formation. For *T* = 277.55 K, *P*<sub>sat</sub> = 3.908 MPa. At *T* and *P*<sub>sat</sub>, liquid volume is 0.04896 L/mol, gas volume is 0.39172 L/mol, and the solubility of CO<sub>2</sub> in seawater with a salinity of 35‰ is 1.50 mol/L. To estimate the solubility of CO<sub>2</sub> at *P* = 8.145 MPa = 80.4 atm, first find liquid CO<sub>2</sub> volume at 8.145 MPa to be 0.04691 L/mol. Using the average liquid volume of (0.04896 + 0.04691)/2 = 0.0479 L/mol, Δ*V* for reaction A3 is -0.0156 L/mol. From 3.908 to 8.145 MPa, -∫Δ*V* d*P*/(*RT*) ≈ 0.0287. Hence, the solubility of liquid CO<sub>2</sub> in seawater at 800 m depth and salinity of 35‰ is 1.55 mol/L.

Knowing CO<sub>2</sub> liquid density (*C*<sub>CO<sub>2</sub>(liq)</sub>) and the solubility of liquid CO<sub>2</sub> (*C*<sub>sat</sub>), the dissolution parameter β<sub>c</sub>, defined in eq 2 as β<sub>c</sub> = (*C*<sub>sat</sub> - *C*<sub>∞</sub>)/(*C*<sub>CO<sub>2</sub>(liq)</sub> - *C*<sub>sat</sub>) where *C*<sub>∞</sub> = 0, can be estimated. Some results are shown in Table 1. The value of β<sub>c</sub> does not change much with depth. For rough calculation, β<sub>c</sub> can be taken as a constant.

In the region of hydrate stability, liquid CO<sub>2</sub> reacts with seawater to form hydrate. A thin hydrate shell would coat the CO<sub>2</sub> droplet. Because CO<sub>2</sub> hydrate is more stable than CO<sub>2</sub> liquid, the dissolution rate of a shelled droplet is smaller. To account for this effect, *C*<sub>sat</sub> in eq 2 should be CO<sub>2</sub> solubility in seawater for hydrate, but *C*<sub>CO<sub>2</sub>(liq)</sub> does not change because the bulk of the droplet is liquid CO<sub>2</sub> and hence *C*<sub>CO<sub>2</sub>(liq with hydrate shell)</sub> is that of liquid CO<sub>2</sub>. At a given *T*, to estimate the CO<sub>2</sub> solubility of CO<sub>2</sub> hydrate, first find the pressure at which CO<sub>2</sub> liquid (or gas) and water are in equilibrium with CO<sub>2</sub> hydrate (Figure 1). At this pressure, the solubility of hydrate is the same as that of CO<sub>2</sub> liquid (or gas). At higher pressures, hydrate solubility depends on volume differences between hydrate and dissolved CO<sub>2</sub>+water. Because hydrate density is about 1100 kg/m<sup>3</sup> (20), increasing pressure would increase the stability of hydrate and decrease its solubility. For the reaction:



where *n* = 7, molar volume is 0.155 L/mol for hydrate and 0.018 L/mol for H<sub>2</sub>O, and 0.0323 L/mol for CO<sub>2</sub>(aq). Hence, Δ*V* for the above reaction is roughly 0.0038 L, so small that hydrate solubility does not decrease much with pressure.

**TABLE 2. Estimation of  $\beta_c$  for the Dissolution of CO<sub>2</sub> Droplet with a Hydrate Shell in Seawater**

temp (K)	depth (m)	density of CO <sub>2</sub> liquid (kg/m <sup>3</sup> )	solubility C <sub>sat</sub> (mol/L)	C <sub>liquid</sub> (mol/L)	$\beta_c$
277.55	800	938	0.944	21.32	0.0463
278.35	600	916	1.000	20.82	0.0504
279.5	400	886	1.084	20.14	0.0569
277.55	3000	1041	0.910	23.65	0.0400
275	3000	1049	0.765	23.84	0.0331

**TABLE 3. Estimation of  $\beta_c$  for the Dissolution of CO<sub>2</sub> Hydrate in Seawater**

temp (K)	depth (m)	density of CO <sub>2</sub> hydrate (kg/m <sup>3</sup> )	solubility C <sub>sat</sub> (mol/L)	C <sub>CO<sub>2</sub>,hydrate</sub> (mol/L)	$\beta_c$
277.55	800	1100	0.944	6.47	0.171

For example, at 277.55 K, CO<sub>2</sub> gas and water react to form hydrate at 2.083 MPa. Hence, hydrate solubility at 2.083 MPa is the solubility of CO<sub>2</sub> gas, which is 0.954 mol/L. As pressure increases from 2.083 to 8.145 MPa, the solubility decreases by only 1%, to 0.944 mol/L. Hence, the effective  $\beta_c$  for a CO<sub>2</sub> liquid drop with a thin hydrate shell is 0.0462 (Table 2). That is, at 4.4 °C, the dissolution rate of liquid CO<sub>2</sub> droplet is 1.69 times that of a shelled CO<sub>2</sub> droplet.

Now the dissolution of a liquid CO<sub>2</sub> layer with a hydrate shell may be compared to that of a solid CO<sub>2</sub> hydrate layer. For the same amount of CO<sub>2</sub>, the volume of CO<sub>2</sub> hydrate is roughly 3.3 times that of CO<sub>2</sub> liquid (because CO<sub>2</sub> hydrate is mostly made of H<sub>2</sub>O). For dissolution of solid CO<sub>2</sub> hydrate, the dissolution parameter  $\beta_c = (C_{sat} - C_{\infty}) / (C_{CO_2(liq)} - C_{sat})$  would be different from that of the shelled CO<sub>2</sub> droplet because now C<sub>CO<sub>2</sub>(liq)</sub> must be replaced by C<sub>CO<sub>2</sub>(hydrate)</sub>. For a density of 1100 kg/m<sup>3</sup>, C<sub>CO<sub>2</sub>(hydrate)</sub> = 6.47 mol/L. At 277.55 K and 800 m depth,  $\beta_c = 0.171$  (Table 3), about 3.7 times  $\beta_c$  for CO<sub>2</sub> liquid with hydrate shell. Because the volume difference is 3.3 and the difference in  $\beta_c$  is 3.7, the dissolution of a layer of the same amount of CO<sub>2</sub> would take roughly the same amount of time whether CO<sub>2</sub> is in the form of liquid with only a hydrate shell, or CO<sub>2</sub> liquid is completely converted to CO<sub>2</sub> hydrate. The thicker layer of CO<sub>2</sub> hydrate would take slightly less time to dissolve.

### Literature Cited

- (1) Marchetti, C. *Clim. Change* **1977**, *1*, 59–68.
- (2) Herzog, H.; Golomb, D.; Zemba, S. *Environ. Prog.* **1991**, *10*, 64–74.

- (3) Eliasson, B.; Riemer, P.; Wokaun, A., Eds. *Greenhouse Gas Control Technologies*; Pergamon: Amsterdam, Netherlands, 1999.
- (4) Alendal, G.; Drange, H. *J. Geophys. Res.* **2001**, *106*, 1085–1096.
- (5) Drange, H.; Alendal, G.; Johannessen, O. M. *Geophys. Res. Lett.* **2001**, *28*, 2637–2640.
- (6) The Royal Society. *Ocean acidification due to increasing atmospheric carbon dioxide*, 2005; <http://www.royalsoc.ac.uk/document.asp?id=3249>.
- (7) Brewer, P. G.; Friederich, G.; Peltzer, E. T.; Orr, F. M., Jr. *Science* **1999**, *284*, 943–945.
- (8) Brewer, P. G.; Peltzer, E. T.; Friedrich, G.; Rehder, G. *Environ. Sci. Technol.* **2002**, *36*, 5441–5446.
- (9) Broecker, W. S.; Peng, T. *Tracers in the Sea*; Lamont-Doherty Geological Observatory: Palisades, NY, 1982.
- (10) Santschi, P. H.; Anderson, R. F.; Fleisher, M. Q.; Bowles, W. J. *Geophys. Res.* **1991**, *96B*, 10641–10657.
- (11) Leifer, I.; Patro, R. K.; Bowyer, P. J. *Atmos. Ocean Technol.* **2000**, *17*, 1392–1402.
- (12) Opdyke, B. N.; Gust, G.; Ledwell, J. R. *Geophys. Res. Lett.* **1987**, *14*, 1131–1134.
- (13) Shafer, N. E.; Zare, R. N. *Phys. Today* **1991**, *44*, 48–52.
- (14) Zhang, Y.; Walker, D.; Leshner, C. E. *Contrib. Mineral. Petrol.* **1989**, *102*, 492–513.
- (15) Kerr, R. C. *J. Fluid Mech.* **1994**, *280*, 287–302.
- (16) Kerr, R. C. *Contrib. Mineral. Petrol.* **1995**, *121*, 237–246.
- (17) Zhang, Y.; Xu, Z. *Earth Planet. Sci. Lett.* **2003**, *213*, 133–148.
- (18) Clift, R.; Grace, J. R.; Weber, M. E. *Bubbles, Drops, and Particles*; Academic Press: New York, 1978.
- (19) Levich, V. G. *Physicochemical Hydrodynamics*; Prentice-Hall: Englewood Cliff, NJ, 1962.
- (20) Aya, I.; Yamane, K.; Nariai, H. *Energy* **1997**, *22*, 263–271.
- (21) Kling, G. W.; Clark, M. A.; Compton, H. R.; Devine, J. D.; Evans, W. C.; Humphrey, A. M.; Koenigsberg, E. J.; Lockwood, J. P.; Tuttle, M. L.; Wagner, G. N. *Science* **1987**, *236*, 169–175.
- (22) Sigurdsson, H.; Devine, J. D.; Tchoua, F. M.; Presser, T. S.; Pringle, M. K. W.; Evans, W. C. *J. Volcanol. Geotherm. Res.* **1987**, *31*, 1–16.
- (23) Zhang, Y. *Nature* **1996**, *379*, 57–59.
- (24) Zhang, Y. *Geophys. Res. Lett.* **2003**, *30*, (51-1)–(51-54).
- (25) Angus, S.; Armstrong, B.; de Reuck, K. M. *International Thermodynamics Tables of the Fluid State: Carbon Dioxide*; Pergamon Press: Oxford, 1976.
- (26) Tamimi, K.; Rinker, E. B.; Sandall, O. C. *J. Chem. Eng. Data* **1994**, *39*, 330–332.
- (27) Weiss, R. F. *Mar. Chem.* **1974**, *2*, 203–215.
- (28) Duan, Z.; Sun, R. *Chem. Geol.* **2003**, *193*, 257–271.

Received for review January 21, 2005. Revised manuscript received July 22, 2005. Accepted July 26, 2005.

ES050140E